Hydrol. Earth Syst. Sci. Discuss., 4, 3583–3626, 2007
www.hydrol-earth-syst-sci-discuss.net/4/3583/2007/

Hydrology and Earth System Sciences Discussions

Papers published in *Hydrology and Earth System Sciences Discussions* are under open-access review for the journal *Hydrology and Earth System Sciences*

An integrated model for the assessment of global water resources – Part 2: Anthropogenic activities modules and assessments

N. Hanasaki[1], S. Kanae[2], T. Oki[2], and N. Shirakawa[3]

[1]National Institute for Environmental Studies, Japan
[2]Institute of Industrial Science, The University of Tokyo, Japan
[3]Graduate School of Systems and Information Engineering, University of Tsukuba, Japan

Received: 17 September 2007 – Accepted: 26 September 2007 – Published: 2 October 2007

Correspondence to: N. Hanasaki (hanasaki@nies.go.jp)

Abstract

To assess global water resources from the perspective of subannual variation in water resources and water use, an integrated water resources model was developed. In a companion report, we presented the global meteorological forcing input used to drive the model and two natural hydrological cycle modules, namely, the land surface hydrology module and the river routing module. Here, we present the remaining four modules, which represent anthropogenic activities: a crop growth module, a reservoir operation module, an environmental flow requirement module, and an anthropogenic withdrawal module. In addition, we discuss the results of a global water resources assessment using the integrated model. The crop growth module is a relatively simple model based on heat unit theory and potential biomass and harvest index concepts. The performance of the crop growth module was examined extensively because agricultural water comprises approximately 70% of total water withdrawal in the world. The estimated crop calendar showed good agreement with earlier reports for wheat, maize, and rice in major countries of production. The estimated irrigation water withdrawal also showed fair agreement with country statistics, but tended to underestimate countries in the Asian monsoon region. In the reservoir operation module, 452 major reservoirs with more than 1 km^3 each of storage capacity store and release water according to their own rules of operation. Operating rules were determined for each reservoir using an algorithm that used currently available global data such as reservoir storage capacity, intended purposes, simulated inflow, and water demand in the lower reaches. The environmental flow requirement module was newly developed based on case studies from around the world. The integrated model closes both energy and water balances on land surfaces. Global water resources were assessed on a subannual basis using a newly devised index that locates water-stressed regions that were undetected in earlier studies. These regions, which are indicated by a gap in the subannual distribution of water resources and water use, include the Sahel, the Asian monsoon region, and southern Africa. The integrated model is applicable to assess various global environ-

mental projections such as climate change.

1 Introduction

Previous assessments of global water resources have projected current and future global water stress, focusing mainly on the spatial, rather than temporal, distribution of water resources and water use. A typical approach is to display the global distribution of per capita annual water resources (Arnell, 1999, 2004) or the withdrawal to water resources ratio on an annual basis (Vörösmarty et al., 2000; Oki et al., 2001; Alcamo et al., 2003a, b). However, extreme seasonality in both water resources and water use occurs in some parts of the world. Therefore, subannual variability must be taken into account. In this two-feature report, we introduce an integrated global water resources model and assess global water resources through the application of the model from the perspective of subannual variation.

We developed an integrated global water resources model with six modules: land surface hydrology, river routing, crop growth, reservoir operation, environmental flow requirements, and anthropogenic water withdrawal. The model simulates both natural and anthropogenic water flow globally (excluding Antarctica) at a spatial resolution of 1°×1° (longitude and latitude). The companion report (Hanasaki et al., 2007) presented two modules of the integrated model, i.e., the land surface hydrology module and the river routing module, which simulate the natural hydrological cycle and the global meteorological forcing inputs that drive the model. Here, we present four modules of the integrated water resources model and discuss the results of global water resources assessments using the integrated model. The model represents anthropogenic activities using a crop growth module, a reservoir operation module, an environmental flow requirement module, and an anthropogenic withdrawal module. These four modules of the integrated water resources model are presented (Sect. 2). The simulation design and the methodology for coupling the six modules together is then described (Sect. 3). The simulation results of four submodules are validated (Sect. 4). Finally, the results of

the global water resources assessment are presented (Sect. 5).

2 The modules

2.1 Crop growth module

Estimating agricultural water demand is particularly important in global water resources assessments because 85% of consumptive water is used for agriculture (Shiklomanov, 2000), with considerable seasonality because the water is needed only during cropping periods. Many crop growth models have been developed, with wide variation in objectives, complexity, and spatiotemporal scales, but a limited number of published studies have applied such models globally in the context of water resources assessment. (Döll and Siebert, 2002) applied basic formulations of the CROPWAT model (Smith, 1992) to estimate annual irrigation water requirements at a 0.5°×0.5° spatial resolution globally. The CROPWAT model is a computer program that calculates irrigation requirements during a prescribed cropping period. Irrigation water requirements are calculated basically from the difference between the amount of water that is needed for optimal crop growth and the effective precipitation during the cropping period (from the planting date to the harvesting date). Although the model is simple and easy to maintain, the cropping period information, which directly affects irrigation water requirements, should be prepared globally. Given limited available data, (Döll and Siebert, 2002) used two crop types and fixed the cropping period at 150 days globally to find the best cropping period (150 sequential days per year) suited for crop growth. Tan and Shibasaki (2003) integrated the Erosion Productivity Impact Calculator (EPIC; (Williams, 1995) with Geographical Information Systems (GIS) and estimated current (2000) and future (2010–2050, including the effects of global warming) crop productivity globally. Contrary to the CROPWAT model, the EPIC model considers crop growing processes in detail; consequently, it allows the simulation of harvesting date, cropping period, and yield for a wide variety of crop species. In the simulation of Tan and Shibasaki (2003),

an irrigation water requirement was calculated, but unfortunately it was neither reported nor validated.

We coded a crop growth module with reference to the Soil Water Integrated Model (SWIM; Krysanova et al., 1998, 2000). The SWIM model is an eco-hydrological model for regional impact assessments in mesoscale watersheds (100–10 000 km^2). The model integrates hydrology, vegetation, erosion, and nitrogen dynamics at the watershed scale. We used only the formulation and parameters of crop vegetation. Because the SWIM model is a descendant of the EPIC model (Williams, 1995) and the Soil Water Assessment Tool (SWAT) model (Neitsch et al., 2002), the formulation and parameters of the crop module are quite similar to those of the earlier models. A description of this module is provided in Appendix A.

Calculations were carried out at daily intervals within each 1°×1° grid cell. The module requires four input hydrometeorological variables: daily temperature (for heat unit and heat stress calculation), shortwave radiation (for photosynthesis calculation), evaporation, and potential evaporation (for water stress calculation). The latter two variables were shared with the land surface hydrology module. The SWIM model can deal with >50 types of crops. For 18 of these crop types, Leff et al. (2004) provide the global distribution of the areal proportion at a 0.5°×0.5° spatial resolution. The remaining crops were simulated using a generic parameter set. The planting date was estimated by conducting a special simulation (described in detail in Sect. 3).

The agricultural water demand was assumed to be equal to the volume of water needed to maintain soil moisture at 75% of field capacity in irrigated fields. Above this threshold, the land surface hydrology module's evaporation becomes identical to the potential evaporation, and consequently, the water stress factor of the crop growth module becomes zero (Hanasaki et al., 2007). In the case of rice, soil moisture was maintained at saturation water content to express inundated conditions. Irrigation began 30 days prior to the planting date, increasing soil moisture content linearly from 0% to 75%. Otherwise, heavy irrigation was required at the planting date to increase soil moisture to at least 75%, especially in arid areas. To identify the proportion of irrigated

area in each grid cell, the global map of Döll and Siebert (2000) was used. Their map has a spatial resolution of 0.5°×0.5° with its original land–sea mask. It was re-gridded to 1°×1° spatial resolution with the common GSWP2 land–sea mask (Dirmeyer et al., 2006) used in this model.

2.2 Reservoir operation module

More than 45 000 large dams have been constructed in the world and their storage capacity exceeds 7000 km^3 in total. Nonetheless, a limited number of studies have focused on the role of reservoirs in global-scale hydrology and water resources modeling (Hanasaki et al., 2006). Earlier studies of global hydrological modeling incorporating reservoirs can be categorized into three groups: 1) those with hydrological models lacking the effects of reservoirs on streamflow simulation (Vörösmarty et al., 1997), 2) those with altered streamflow simulation based on a formulation common to that of natural lakes (Meigh et al., 1999; Döll et al., 2003), and 3) those with altered streamflow simulation based on a formulation quite different from that of natural lakes (Haddeland et al., 2006a, b; Hanasaki et al., 2006). The reservoir operation scheme of Haddeland et al. (2006b) and Haddeland et al. (2006a) is a retrospective approach requiring two runs per simulation. First, they ran their global hydrological model to simulate global streamflow without reservoir operations; then an optimal reservoir operation (series of release and storage controls throughout a year) was searched to maximize the utility function (specific to the reservoir's primary purpose). In this approach, the reservoir operating rule is based on perfect information of inflow and water use in the lower reach of the year. In contrast, the scheme of Hanasaki et al. (2006) is a forward approach that generates future operating rules with just one estimate per year. We used the reservoir operation scheme developed by Hanasaki et al. (2006).

In the global river map of the river routing module, the 452 largest reservoirs with storage capacity >10^9 m^3 each worldwide were geo-referenced, and available reservoir information (e.g., name, purposes in order of priority, and storage capacity) was compiled (Hanasaki et al., 2006). The total storage capacity of these 452 reservoirs

was 4140 km^3, accounting for approximately 60% of the total reservoir storage capacity in the world. The reservoir operation module set operating rules for individual reservoirs. For reservoirs for which the primary purpose was not irrigation water supply, the reservoir was operated to minimize interannual and subannual streamflow variation for its condition (i.e., storage capacity and inflow). For reservoirs for which the primary purpose was irrigation water supply, daily release from the reservoir was proportional to the irrigation water requirement in the lower reaches. A detailed description of the reservoir operation module is provided in Appendix B.

2.3 Environmental flow requirement module

Global modeling of environmental flow requirements is a relatively new topic in global hydrology. Smakhtin et al. (2004) reported the estimation of global environmental requirements at a spatial resolution of 0.5°×0.5°. They defined the annual environmental flow requirement as the sum of the low flow requirement (LFR) and the high flow requirement (HFR). They used the concept of a flow duration curve. They argued that to maintain the conservation status of management objectives to fair conditions (moderately or considerably modified), LFR should exceed Q90 streamflow (90th percentile streamflow), Q75 for good conditions, and Q50 for natural (unmodified) conditions. They set HFR according to the relationship between mean annual streamflow and Q90 (Table 1). These criteria allocated 20% to 50% of the mean annual river flow as the sum of LFR and HFR or to freshwater-dependent ecosystems to maintain them in fair condition.

W estimated a monthly environmental flow requirement using the algorithm of Shirakawa (2005, 2004). We did not insist that the environmental flow requirement estimated by this algorithm be sufficient for aquatic ecosystems. Unless withdrawal from and pollution of rivers is prohibited, the ecosystem is more or less affected and changed by human activities. Whether the change or damage is tolerable or not is highly dependent on value judgments of society. The algorithm was based on case studies

and fieldwork in semiarid to arid regions or in heavily populated regions, which provide actual examples of value judgments in relatively water-scarce regions. There is no universal theory regarding environmental flow requirements. Indeed, value judgments are largely influenced by regional welfare and culture. However, because of limited information regarding global applicability, the algorithm only accounted for natural hydrological conditions; cultural and economic perspectives were not considered.

Because both (Shirakawa, 2005, 2004) were published in Japanese, we describe Shirakawa's methodology. First, using the 10-year mean monthly gridded streamflow data simulated by the land surface hydrology module and the river routing module, all grids were classified into four regions following the criteria in Table 2. The environmental flow requirement consisted of two factors: the base requirement, which showed minimum streamflow in the channel; and the perturbation requirement, which allowed flush streamflow in the rainy season. The perturbation requirement was 10% of the mean monthly streamflow and should be run in two or three days. However, taking into account the current spatiotemporal resolution of this study, the perturbation requirement was not implemented; instead, the allocated amount was simply added to the base requirement.

The 10% and 30% thresholds of base requirements are based on the work of Tennant (1976). He evaluated environmental flow as a proportion of mean annual streamflow and argued that 10% was the minimum requirement, 30% was good, and 60% was excellent. A threshold of 30% was further supported by a number of studies. King et al. (2000) introduced some case studies of rivers in South Africa and argued that the annual total environmental flow was 37.3–45.7% of the annual streamflow for the Marite River and 30.2% for the Mhlatuze River. The water plan of the state of California, USA, projected the future share of water use by sector and argued that the environmental flow requirements will be 32–46% of the total water demand in 2020 (Department of Water Resources State of California, 1998). In Japan, the environmental flow requirement was determined from several thresholds such as the 1) Q_{97} streamflow (355 of 365 days exceed the streamflow; given the national average of 284 mm yr^{-1},

approximately 25% of mean annual streamflow; (Japan River Association, 2007); 2) 95 mm yr^{-1} (8%) for rivers below hydropower reservoirs (Ministry of Land Infrastructure and Transportation, 2001); and 3) 218 mm yr^{-1} (18%) for the remaining rivers (a government notification of Ministry of Construction issued in 1988). However, it has been argued that these Japanese thresholds are too small to maintain aquatic ecosystems. Taking these earlier studies into account, we judged 30% of the mean annual inflow to be a good criterion for the environmental flow requirement.

Four major features are common to the algorithm of Smakhtin et al. (2004) and our algorithm: 1) both are based on monthly streamflow data for more than one year, 2) both use the sum of low flow and high flow to deal with seasonal streamflow variability, 3) both account for the regional hydrological regime, and 4) both are designed for a universal model that is applicable worldwide. In contrast, our environmental flow requirement module differs from that of Smakhtin et al. (2004) in five ways: 1) a monthly streamflow field is used instead of Q90, 2) the environmental flow requirement is calculated on a monthly basis with seasonality, 3) a zero requirement is allowed in dry regions, 4) regional classification is based not only on aridity (dry and wet) but also on temporal stability (stable and variable), and 5) the environmental flow requirement is based on case studies and fieldwork performed primarily in semi-arid or densely populated regions.

2.4 Anthropogenic water withdrawal module

The anthropogenic water withdrawal module withdraws the consumptive amount of domestic, industrial, and agricultural water from river channels in that order at each simulation grid cell. This module plays an important role in coupling water fluxes among the land surface hydrology, river routing, crop growth, and environmental flow requirement modules.

Domestic and industrial water use was not estimated by the integrated model. Instead, it was obtained from the AQUASTAT database (Food and Agriculture Organization, 2007a). The AQUASTAT database provides statistics-based national water

withdrawal for domestic, industrial, and agricultural sectors. It was converted to gridded data by weighting the population distribution and national boundary information provided by the Center for International Earth Science Information Network (CIESIN) Columbia University and Centro Internacional de Agricultura Tropical (CIAT) (2005). It was then converted to the consumptive amount, which is the evaporated portion of the total withdrawal. We used 0.10 for domestic water and 0.15 for industrial water, from the study of Shiklomanov (2000). Seasonal variation was not taken into account for these water uses.

When streamflow was less than the total water demand, streamflow except for the share of environmental flow, was withdrawn. Withdrawn irrigation water was added to the soil moisture in irrigated areas, and domestic and industrial waters were removed from the system. This latter process was an exception to the closure of the energy and water balance; however, the sum of consumptive domestic and industrial water was 132.4 $km^3\,yr^{-1}$ in 1995 (Shiklomanov, 2000). This amount was two orders of magnitude less than global runoff and evaporation (40 000 $km^3\,yr^{-1}$ and 71 000 $km^3\,yr^{-1}$, respectively (Baumgartner and Reichel, 1975), and was thus judged to be negligible.

3 Simulation

3.1 Input data

To drive the integrated model, we used the meteorological forcing input F-GSWP2-B1, which is described in detail in the companion paper (Hanasaki et al., 2007). It consists of seven variables: air temperature, specific humidity, wind speed, air pressure, downward shortwave radiation, downward longwave radiation, and precipitation. All variables are three hourly from 1 January 1986 to 31 December 1995 at a spatial resolution of 1°×1°. The meteorological forcing input is a hybrid product of ground observation-based monthly gridded data and temporally high-resolution reanalysis data. The precipitation in Europe has overestimation bias, especially at high latitudes; consequently,

evaporation and runoff are higher than in earlier studies. This is attributed to the rain gauge undercatch correction applied to the precipitation forcing input (see Hanasaki et al., 2007, for details).

3.2 Integration of the modules

In this section, the coupling of the six modules is described (Fig. 1a). First, the land surface hydrology module is called to calculate energy and water balances on land surfaces. Next, the crop growth model is called. The input shortwave radiation and air temperature are identical to those of the land surface hydrology module, and evaporation and potential evaporation are the simulated results of the land surface hydrology module. Consumptive agricultural water demand is estimated during the cropping period. Runoff is routed by the river routing model, and streamflow is calculated. This calculation is conducted from upper stream grids to lower stream grids; if reservoirs are geo-referenced in the calculated grid cells, the reservoir operation module is called to calculate release, storage, and altered streamflow. The environmental flow module simulates the monthly environmental flow requirement from the monthly runoff. Finally, the anthropogenic water withdrawal module links water demand and streamflow. It withdraws domestic, industrial, and agricultural water from streamflow in this order. Withdrawal is controlled to remain at or above the environmental flow requirement. The agricultural water withdrawn is added to the soil moisture of irrigated lands, and the domestic and industrial water withdrawn is removed from the integrated model system (i.e., it disappears without closure of water and energy balances on land surfaces). In reality, some portion of withdrawn water evaporates (water consumption) and the remaining portion returns to rivers or aquifers (return flow). For simplicity, this model takes only consumptive water into account, and only the consumptive portion is withdrawn from the water source.

The basic calculation time step of the model is one day. The land surface hydrology and river routing modules are exceptions; they simulate at three-hour intervals determined by the meteorological forcing data. Also, the environmental flow requirement

module operates on a monthly time step. One might consider a $1^\circ \times 1^\circ$ spatial resolution too coarse for daily calculations. In equatorial low latitudes, 1° in longitude corresponds to approximately 120 km, and the length of river channels in the river routing module is 120 km$\times$1.4$\approx$170 km (1.4 expresses the meander of rivers in real conditions; Oki and Sud, 1998). The flow velocity of the river routing module is 0.5 m s^{-1}; therefore, roughly speaking, a river flows through a grid in approximately four days. In this context, $0.25^\circ \times 0.25^\circ$ spatial resolution is suited for daily calculations; however, because of limited global meteorological forcing data, this is simply not feasible. Therefore, the $1^\circ \times 1^\circ$ resolution is a bit coarse for daily simulations, but we judged it to be a feasible and reasonable alternative.

3.3 Assumptions

The simulations were carried out under three important assumptions. First, water is withdrawn only from river channels. In reality, groundwater, lakes, ponds, and glacial meltwater are major sources of water in some parts of the world. These nonriver water resources can be divided into renewable and nonrenewable components. For example, withdrawal from shallow groundwater, lakes, and ponds below the recharge rate is considered renewable. In contrast, withdrawal from deep groundwater, glacial meltwater, and overexploitation of lakes and ponds is considered nonrenewable. The renewable water resources are partly included in this simulation because simulated runoff and streamflow are the result of water balance calculations on land surfaces, and the natural recharge of groundwater in lakes and ponds is implicitly included in the runoff. This does not apply to nonrenewable water resources, and they are excluded from this simulation. Therefore, the simulated availability of water might be underestimated, especially in areas that rely heavily on nonrenewable water resources; the water use in these areas can be considered less sustainable and vulnerable to water scarcity.

Second, only consumptive water is withdrawn from river channels. In reality, a considerable amount of withdrawn water does not reach the destination because of evaporation and percolation losses during delivery. Also, a considerable portion of withdrawn

water is returned to the river through drainage channels and groundwater flow. Consequently, the simulated water demand is underestimated. Part of the return flow is implicitly expressed by a simple subsurface flow scheme in the land surface module, and a portion of irrigated water is drained and returned to the river.

Third, a simplified cropping pattern is assumed because of limited detailed information on global cropping practices. We assumed that the same crop species is planted in both irrigated and nonirrigated croplands. The global distribution of crop species was obtained from Leff et al. (2004). To further simplify the simulation, only information on primary and secondary crop types in terms of the cultivated area of Leff et al. (2004) was used. We then assumed that the primary crop was cultivated as the first crop and the secondary crop was cultivated as the second crop. The crop intensity of irrigated cropland (the areal proportion of cultivated area to the total irrigated area) was obtained from Döll and Siebert (2002). According to their estimation, crop intensity varied from 0.8 (on average, 80% of the total irrigated cropland is used) in parts of the former USSR, Baltic States, and Belarus to 1.5 in eastern Asia, Oceania, and Japan. In these cases, we assumed that only 80% of the irrigated land was cultivated in the first crop and no second crop was planted in the former group of countries, whereas cultivation is 100% for the first crop and 50% for the second crop for the latter group of countries.

3.4 Integration of simulations

To run the fully coupled global water resources model, a series of simulations is required (Fig. 1b). First, the land surface hydrology module and the river routing module were coupled and a global natural hydrological simulation was conducted (hereafter "NAT simulation", short for natural hydrological cycle simulation). The purpose of this simulation was to obtain long-term mean hydrological variables and to prepare essential information for other modules. These items included mean annual streamflow for the reservoir operation module, mean monthly runoff for the environmental flow requirement module, and mean daily evaporation and potential evaporation for crop calendar estimation.

Second, a global cropping calendar was estimated by conducting a special simulation using the crop growth module (hereafter "CAL simulation", short for crop calendar estimating simulation). In this simulation, four hydrometeorological inputs were used: mean daily air temperature, shortwave radiation, evapotranspiration, and potential evapotranspiration. The latter two variables were obtained from the NAT simulation. Then 365 sets of crop yield were calculated for each grid by shifting the starting date of cropping from 1 January to 31 December, and the cropping date that produced the largest yield in a year was determined. If the temperature in the cropping period fell below the base temperature (*TB* in Eq. A1), the crop was killed and its crop yield was zero, except for winter crops. The cropping calendar for double crops was also estimated for the remaining noncropping period so as not to overlap the period during the planting date and harvesting date of the first crop. The minimum interval between two cropping periods was set at 15 days. This simulation was conducted for all 19 types of crops (18 specific crop types and one generic crop parameter).

Third, a special simulation was conducted to estimate irrigation water demand. The land surface hydrology and crop growth modules were coupled, and a global hydrological simulation was conducted for 10 years from 1986 to 1995 (hereafter "IRG simulation", short for ideally irrigated simulation). In this simulation, water balance was ignored, and ideal irrigation water was applied to the irrigated cropland during the cropping period. As described in Sect. 2.1, the irrigation water requirement was calculated from the deficit of soil moisture in irrigated fields during the cropping period. This amount of water corresponded to the consumptive irrigation water demand. In this simulation, the crop calendar estimated in the CAL simulation was used.

Finally, all six modules were coupled, and global water resources were simulated from 1986 to 1995 (hereafter "FUL simulation", short for fully coupled simulation). For all simulations, the meteorological input for the first year of the simulation period was iteratively given to the coupled model until soil moisture, river channel water storage, and reservoir storage reached equilibrium. A 10-year simulation was then conducted. In this simulation, the crop calendar estimated in the CAL simulation was used.

4 Validation

In this section, the crop growth module and environmental flow requirement module are validated and compared with earlier studies. The validation of the reservoir operation module is omitted because it has already been described elsewhere (Hanasaki et al., 2006). The withdrawal module is also omitted because it couples the water fluxes of five modules, but does not generate any new variables.

4.1 Crop calendar

Because agricultural water occupies 66% of the total water withdrawal and 85% of the total water consumption (Shiklomanov, 2000), the estimation of the timing and amount of the agricultural water requirement is critical in water resources assessment. The estimated crop calendar was compared with earlier work by the World Agricultural Outlook Board U.S. Department of Agriculture (1994) (hereafter WAOB94). It provides the planting and harvesting dates of major crops for major countries of the world. We compiled planting dates and harvesting dates of three major grains, namely, wheat, maize, and rice, for 10 countries with the highest production in the world in 2000 (Food and Agriculture Organization, 2007b; Fig. 2). WAOB94 normally provides one general cropping calendar for a country, and both planting date and harvesting date have a wide range of up to four months.

Wheat is the most widely planted crop in the world (Ishii et al., 1999). Cropping can be roughly divided into two patterns: spring wheat, which is planted in spring and harvested in autumn; and winter wheat, which is planted in autumn and harvested in early summer (Fig. 2a). For spring wheat, both the simulated planting dates and harvesting dates in the USA, Canada, and Russia generally agreed with those of WAOB94. For China, the simulated cropping period was reproduced, but both the planting date and the harvesting date were approximately one month later than those of the WAOB94. For winter wheat, the simulated planting dates were reproduced fairly well, except for China and India, whereas the simulated harvesting dates were sometimes one month

(Russia, Britain) to two months (France, Germany) earlier than those of the WAOB94.

The planting dates of winter wheat in China and India were split into two groups: one resembled winter wheat and the other resembled spring wheat. This variation reflected differences in regional performance. In India, the simulated planting date of northwestern India agreed well with the observations, but in north-central to northeastern India, the simulated planting date was two to three months earlier than in the WAOB94. In China, the simulated planting date of the southern North China Plain was simulated, but the remaining areas such as the Sichuan Basin and central North China Plain had a simulated crop calendar that resembled spring wheat; however, in reality, winter wheat was expected. These erroneous simulated planting periods were caused by water stress during the cropping period. In both China and India, low precipitation in winter restricted the crop yield of winter wheat to levels below those of spring wheat. We estimated the planting date under ideal water conditions (i.e., no water stress during the cropping period). In this case, the planting date was well reproduced (not shown). In these regions, the cropping calendar could be improved by irrigation.

For maize, the planting dates in major cropping countries, namely, the USA, China, Brazil, and Mexico were well reproduced (Fig. 2b). Harvesting dates were also well reproduced in China and Brazil, but they were approximately one month earlier in the USA and Mexico (Fig. 2b). The estimated planting and harvesting dates in Argentina varied, but the planting dates were about one month later than the observed dates. In France and Italy, both planting dates and harvesting dates were reproduced. In India and South Africa, the cropping period was one to two months shorter than in the WAOB94, but the general pattern was captured. In Indonesia, the simulated cropping period was quite different from that of the WAOB94.

FAOSTAT reports that Vietnam and the Philippines ranked sixth and ninth in rice production in 2000, respectively. Nonetheless, these countries were omitted from the planting dates and harvesting dates for rice in 10 major countries because Vietnam extends north and south and the WAOB94 shows wide variation in the rice crop calendar, and the Philippines' land area was not properly set in our simulation because of the

coarse land and sea distribution of GSWP2. More than 90% of rice is produced in the Asian monsoon region (Ishii et al., 1999). The simulated planting dates and harvesting dates were captured in the 10 selected countries (Fig. 2c). In the top three countries, i.e., China, India, and Indonesia, both the planting date and harvesting date agreed with observations in most of these areas. There were exceptional grids with large differences from observations, but most of them were attributed to the vast climate region of these countries because they are at the margins of the major cropping areas. The cropping patterns of Bangladesh and Brazil were captured. In Japan and the USA, both the simulated planting dates and harvesting dates shifted one month earlier than in WAOB94. The planting date in Pakistan was captured, but the harvesting date was approximately one-half to one month earlier than in the WAOB94. In Thailand and Myanmar, the planting date was estimated to be one to two months earlier and the cropping period was shorter than in WAOB94. In these countries, floodwater inundates paddy fields, but this process was not incorporated in our system.

In general, the planting dates and harvesting dates of major crops in major cultivation areas agreed with the WAOB94, but there was a tendency toward the early estimation of planting dates, and the cropping periods were shorter than in WAOB94. This tendency was noticeable in countries that have warmer climates such as India, Brazil, and southeastern Asian countries, rather than those that have colder climates such as European countries.

4.2 Irrigation water demand

The crop growth module estimated the consumptive water requirement, but most of the available statistics reported water withdrawal, which includes loss during delivery and return flow to the river channel or the recharge of groundwater. We used the methodology of Döll and Siebert (2002) to convert the consumptive water requirement ($Q_{\text{consumptive}}$) to a withdrawal basis ($Q_{\text{withdrawal}}$). They defined the irrigation efficiency

(k_{eff}; range from 0 to 1) as:

$$k_{\text{eff}} = Q_{\text{consumptive}} / Q_{\text{withdrawal}} \quad (1)$$

They compiled k_{eff} for 19 countries and regions worldwide. It ranges from 0.35 to 0.70, reflecting irrigation facilities and practices. Table 3 shows irrigation water withdrawal estimates from earlier studies for each continent. The estimates of global total irrigation water withdrawal ranged from 2020 km yr^{-1} to 2660 km yr^{-1}, but except for a study of the World Resources Institute (WRI) (1998), the range was 2500±150 km yr^{-1}. Our estimation (2810 km yr^{-1}) slightly exceeds the upper limit of this range, but still reasonable.

A country-based comparison of irrigation water withdrawal with the AQUASTAT database (Food and Agriculture Organization, 2007a) for 127 countries is provided (Fig. 3). For countries with irrigation water demand >100 km^3 yr^{-1}, China and the USA were reproduced well and were within the range between +25% and −20%. India was overestimated at slightly more than +25%, and Pakistan was overestimated considerably at almost twice the expected value. Countries with irrigation water demand between 30 km^3 yr^{-1} and 100 km^3 yr^{-1}, can be categorized into two groups: Asian monsoon countries, i.e., Thailand, Bangladesh, Indonesia, Japan, Vietnam, and Myanmar; and the remaining countries, i.e., Iran, Mexico, Uzbekistan Republic, Egypt, Iraq, Brazil, and Sudan. Irrigation water withdrawal for the Asian monsoon countries was significantly underestimated, except for Thailand and Myanmar. It is interesting that these countries are all major rice producing countries (see Fig. 2c). In irrigated paddy rice fields, extra water may be used by farmers to enhance crop growth and to avoid weeds and low-temperature stress (Ishii et al., 1999), which was not included in the model. Except for Asian monsoon countries, three of seven countries came within +25% to −20% of the expected value, and five of seven countries came within +100% to −50%. Taking into account the limited reliability of available irrigation information, we judged the estimates to be tolerable.

4.3 Environmental flow requirement

Because there are no observations of environmental flow requirements, the estimated results of the environmental flow requirement module were compared with the earlier study of Smakhtin et al. (2004). Using the simulated streamflow of the NAT simulation, two annual environmental flow requirements were simulated using the environmental flow requirement module and the methodology of Smakhtin et al. (2004) (Fig. 4).

The simulated environmental flow requirement ranged from 0% to 40% of the total mean annual runoff (Fig. 4a). The minimum of 0% was allocated if the monthly runoff fell below 1 mm mo^{-1} throughout a year, and it occurred mainly in arid areas. The maximum of 40% was allocated if the monthly runoff exceeded 10 mm mo^{-1} throughout a year. The total environmental flow requirement was estimated at 12 492 km^3 yr^{-1}, approximately 32% of the global total runoff of the NAT simulation. The global distribution pattern of the environmental flow requirement was quite similar to that of runoff.

In contrast, the global distribution of Smakhtin et al. (2004) was quite different; for most regions of the world, it ranged between 20% and 30% of the mean annual runoff. The low regional variation was inherent in their classification and allocation of environmental flow requirements (Table 1). The total environmental flow requirement was 10 682 km^3 yr^{-1}, approximately 27% of the global total runoff. The results clearly show that the method that we used (Shirakawa, 2004, 2005) produced less environmental flow in arid to semi arid areas and more in tropical areas. The distribution (Fig. 4b) is different from that of the original publication (Smakhtin et al., 2004) because the former was calculated from the runoff of the NAT simulation, whereas the latter used the simulated streamflow data of Döll et al. (2003). The environmental flow at high latitudes of North America was much higher in the original publication. The hydrological model of Döll et al. (2003) had a natural lake scheme, which buffered the fluctuation in runoff. The natural lakes abundant in northern North America enlarged the Q90 and the environmental flow requirement calculated by the algorithm of Smakhtin et al. (2004).

5 Results and discussion

A global water resources assessment was conducted using indices. The three indices applied were the withdrawal to water resources ratio, the cumulative withdrawal to water demand ratio, and the consumption to Q90 ratio.

5.1 Conventional index

First, the withdrawal to water resources ratio (hereafter WWR) was calculated as the ratio of annual water withdrawal to annual runoff (renewable freshwater). It was expressed as:

$$\mathrm{WWR} = \frac{W}{Q} \tag{2}$$

where W is the annual total withdrawal and Q is the annual streamflow. The areas with WWR<0.2 had low or no stress; areas with 0.2≤WWR<0.4 had medium stress; and areas with 0.4≤WWR had high stress (Raskin et al., 1997). To exclude sparsely populated deserts, grids with <1 person km^{-2} were masked out of the global distribution of WWR (Fig. 5a). The medium- to high-water-stressed regions extended from western India across the Middle East, northern Africa, the western Great Plains in USA, and northern China to central Asia. This distribution largely agreed with that of earlier studies (e.g., Vörösmarty et al., 2000; Alcamo et al., 2003a, 2007; Oki and Kanae, 2006), indicating that global water resources and water use are well reproduced in our modeling system on an annual basis. For the population living in water stressed areas (0.4≤WWR; Table 4) the stressed population was smaller than that of earlier studies (Vörösmarty et al., 2000; Oki et al., 2001; Alcamo et al., 2007). There are two major reasons for this. First, the spatial resolution was lower than in earlier studies, and consequently the population density was lower. Second, a large area of coastal zone was classified as sea in this simulation because of the characteristics of the land–sea mask of GSWP2. The world population on the land grid was 5195 million in the simulation,

but was reported as 5646 by the Center for International Earth Science Information Network (CIESIN) Columbia University and Centro Internacional de Agricultura Tropical (CIAT) (2005). Not only was the total population smaller, but the population density was higher in coastal zones. As a result, the stressed population was lower than in earlier studies.

5.2 Newly developed index

Here, we propose a new index, the "cumulative withdrawal to demand ratio (CWD)" to express whether water demand is fulfilled on a subannual basis:

$$\mathrm{CWD} = \sum_{Y=1986}^{1995} \sum_{\mathrm{DOY}=1}^{365} w_{Y,\mathrm{DOY}} \Big/ \sum_{Y=1986}^{1995} \sum_{\mathrm{DOY}=1}^{365} d_{Y,\mathrm{DOY}} \tag{3}$$

where $d_{Y,\mathrm{DOY}}$ is the daily water demand (Y: year; DOY: day of year), and $w_{Y,\mathrm{DOY}}$ is the simulated daily water withdrawal from streamflow for each grid. Daily water withdrawal does not exceed daily water demand ($w_{Y,\mathrm{DOY}} \leq d_{Y,\mathrm{DOY}}$). We set the area such that $0.8 \leq \mathrm{CWD}$ indicates low or no stress, $0.5 \leq \mathrm{CWD} < 0.8$ denotes medium stress, and $\mathrm{CWD} \leq 0.5$ represents high stress. These criteria were determined arbitrarily so that the highly stressed areas generally involve a well-established WWR. Figure 5b shows the distribution of the CWD index. Compared to WWR, water stressed regions were expansive.

We examined the relationship between CWD and WWR for all land grids (total of 15 238; Fig. 6a). Of particular note are the plots in which WWR showed low water stress, but CWD showed high water stress. We defined category A as a WWR indicating low to no stress ($0 \leq \mathrm{WWR} < 0.2$) and CWD indicating medium to high stress ($0 \leq \mathrm{CWD} < 0.8$) or a WWR indicating medium stress ($0.2 \leq \mathrm{WWR} < 0.4$) and CWD indicating high stress ($0 \leq \mathrm{CWD} < 0.5$). Category A grids occur in the Sahel region, the Asian monsoon region, including India and Thailand, and southern Africa (Fig. 6c). In these regions, water stress is caused by a gap in the subannual distribution of water

resources and water use, which is overlooked in conventional studies based on WWR alone. In reality, not all of the water is supplied by streamflow. Groundwater, glacial meltwater, and water in lakes or ponds may be important sources. In addition, reservoirs $<10^9$ m^3 that were not included in the model may contribute. The water-stressed regions detected by CWD are likely to rely on nonrenewable water resources or water resources developed by infrastructure such as artificial reservoirs.

5.3 Consumption to Q90 ratio

The consumption to Q90 ratio (hereafter CQ90) was recently proposed by Alcamo et al. (2007) as:

$$C\mathrm{Q90} = \frac{C}{\mathrm{Q90}} \tag{4}$$

where C is consumptive water use and Q90 is the 90th percentile streamflow. They argued that this index is easier to interpret physically than WWR because $\mathrm{CQ90} \geq 1$ implies that the entire low monthly runoff in a river basin is depleted. This index takes the seasonality of water resources into account by using Q90 information. The estimated consumptive water requirement is largely exceeded in the water-stressed region indicated by the WWR, and the stressed region expands to eastern India, part of Southeast Asia, southern China, the Sahel, southern Africa, and eastern South America (Fig. 5c). The distribution is quite similar to that of CWD.

Although CWD (Fig. 5b) and CQ90 (Fig. 5c) show no clear differences in the distribution of water-stressed areas, the relationship between CWD and CQ90 is weak (Fig. 7). Even for grid cells with CQ90 of 100 to 1000, which indicates that the consumptive water demand exceeds the Q90 by 100 to 1000 times, the CWD shows that there are lots of grid cells in the world in which approximately 80% of the daily water demand can be fulfilled. This clearly suggests that even Q90 is far below the annual average consumptive water use; if the water use is concentrated in water-rich periods, the availability can be quite high. The CQ90 indicates water-stressed regions with large

seasonality in water resources; however, it provides little information when it exceeds 1. Although, the estimation of the timing and amount of irrigation water requirements has uncertainty, the CWD gives information on the potential availability of water with strong seasonality in water resources. The CWD may be more informative than the CQ90, for example, in the assessment of the effect on regional water resources of the earlier arrival of streamflow peaks associated with climate change.

5.4 Effect of reservoirs and environmental flow requirements

How important are the operations of the 452 largest reservoirs and environmental flow from a global perspective? Reservoir operation reduces water stress and environmental flow increases water stress because it limits withdrawal from channels. These factors can alter the population under high water stress by approximately 10% (Table 5). Clearly, this number is not negligible for water resources assessments.

6 Conclusions

An integrated water resources model was developed that consists of six modules to simulate both natural and anthropogenic water flows at daily intervals. A global water resources assessment was conducted using a newly devised indicator, the cumulative withdrawal to demand ratio, which detects water-stressed regions that were previously overlooked. For example, a gap in the subannual distribution of water resources and water use was noted in the Sahel, the Asian monsoon region, and southern Africa.

The crop growth module simulates crop yield. Currently, it is used only to estimate crop calendars, but it can be further used for virtual water estimation (Hoekstra and Hung, 2002; Oki and Kanae, 2004). It is also applicable for the impact analysis of water resource shortages on agricultural crop production, which can serve as another water stress index.

Climate change is likely to alter future temperature and precipitation patterns and

in turn alter the availability of renewable freshwater and water use. Our model can contribute to assessments of the effects of global warming on water resources by considering changing variation in precipitation, runoff, and water use. Arnell (2004) pointed out that according to the per capita water availability indicator, climate change would appear to reduce global water stress because increases in runoff are heavily concentrated in the most populous parts of the world, mainly in East and Southeast Asia, and tend to occur during high-flow seasons. Kundzewicz et al. (2007) argued that this might not alleviate dry season problems if the extra water is not stored, and it would not ease water stress in other regions of the world. A global water resources assessment under future global warming will be addressed in forthcoming papers.

Appendix A

Crop growth module

The crop growth module is presented briefly. A full description of the scheme and parameters can be found in Krysanova et al. (2000). The module estimates the cropping period to obtain mature total plant biomass and crop yield. The module estimates crop growth using heat unit theory. After planting, the module accumulates daily heat units (HUNA*(t)*), which are expressed as the daily mean air temperature (T) above the plant's specific base temperature (TB; given as a crop-specific parameter). When the accumulated heat units reach the potential heat units required for the maturity of the crop (PHUN; given as a crop-specific parameter), the crop is mature and is harvested:

$$\mathrm{HUNA}(t) = T - TB \tag{A1}$$

$$\mathrm{IHUN} = \frac{\sum_t \mathrm{HUNA}(t)}{\mathrm{PHUN}} \tag{A2}$$

During the cropping period, plant biomass is calculated using a simple photosynthesis model:

$$\Delta BP = BE \cdot \mathrm{PAR} \tag{A3}$$

$$\mathrm{PAR} = 0.02092\mathrm{RAD}\cdot[1-\exp(-0.65\mathrm{LAI})] \tag{A4}$$

where ΔBP is the daily potential increase in total biomass [kg ha^{-1}], BE is a crop-specific parameter [kg m^2 MJ^{-1} ha^{-1} d^{-1}], PAR is photosynthetically active radiation [MJ m^{-2}], RAD is shortwave radiation [Ly], and LAI is the leaf area index, which is estimated using empirical equations and crop-specific parameters. The four stress factors affecting crop growth are temperature, water, nitrogen, and phosphorous. When air temperature deviates from the crop's optimal temperature or when evaporation is restricted by a lack of soil moisture, the growth of plant biomass is restricted. Nitrogen and phosphorous stress was not considered because of a lack of available information on fertilizer application. The crop yield (YLD; kg ha^{-1}) is estimated by multiplying the harvest index (range from 0 to 1) by the aboveground biomass at the harvesting date:

$$\begin{aligned} &\mathrm{YLD} = \mathrm{HVSTI} \cdot \frac{\mathrm{WSF}}{\mathrm{WSF}+\exp(6.117-0.086\cdot\mathrm{WSF})} \cdot \mathrm{BAG} \\ &\text{where} \quad \mathrm{WSF} = \frac{\mathrm{SWU}}{\mathrm{SWP}} \end{aligned} \tag{A5}$$

where HVSI is a crop-specific parameter, BAG is aboveground biomass [kg ha^{-1}], SWU is the accumulated actual plant transpiration in the second half of the growing season [kg ha^{-1}], and SWP is the accumulated potential evapotranspiration in the second half of the growing season [kg ha^{-1}].

If we use the formulation and parameters of the SWIM model globally, the cropping period of countries at low latitudes become unrealistically short (e.g., <100 days for the cropping period of grains). The SWIM model provides only one parameter set for each crop type, e.g., base temperature, optimal temperature, and potential heat units required for maturity. Heat units accumulate rapidly when the difference between the daily mean temperature and the base temperature is large, and the threshold of

potential heat units required for maturity is attained quickly. Therefore, we set an upper limit for daily heat units. Doorenbos and Pruitt (1977) showed cropping periods for various crops planted in various places in the world; except for some vegetables, crops need at least 120 days to mature. The potential heat unit threshold for maturity is in many cases 1500°K in the SWIM model, so we set the daily maximum heat unit threshold to 12.5°K and excluded any excess heat units. In this case, at least 120 days are needed to reach maturity in all crops. This corresponds to altering the TB in Eq. (A1) to fit the local temperature or to planting different species that have larger a TB than that of SWIM.

Appendix B

Reservoir operation module

This module sets operating rules for individual reservoirs. There are two types of operating rules: irrigation or nonirrigation. If the reservoir's primary purpose is not irrigation water supply, the "nonirrigation operating rule" is set as follows. This operation tries to reduce both the interannual and seasonal variation in streamflow, and if conditions allow, the reservoir releases the mean annual inflow throughout the year. First, for every reservoir-georeferenced grid, each month is categorized as either a recharge month, in which mean monthly inflow exceeds mean annual inflow, or a release month. Second, we define the "operational year," which begins in the first month of a release period (longest continuous release months in a year). We assume that the annual total release for an operational year is fixed at the beginning of the operational year. Thus, the annual total release for the operational year (R [kg yr^{-1}]) is provisionally set as:

$$R \approx \frac{S_{\mathrm{ini}}}{0.85C} \times I_{\mathrm{mean}} \tag{B1}$$

where I_{mean} is the mean annual inflow [kg yr^{-1}], S_{ini} is the storage at the beginning of the operational year [kg], and C is the storage capacity of the reservoir [kg]. The coefficient of 0.85 was set semiempirically (Hanasaki et al., 2006). If storage was smaller than $0.85C$, the release for the next 12 months was smaller than the mean annual inflow to recover storage. In this way, the interannual variation in inflow is buffered by the reservoir. Once the annual release is fixed, the daily release from reservoirs (r [kg s^{-1}]) is expressed as:

$$r = \begin{cases} \frac{S_{ini}}{0.85C} \times i_{mean} & (c \equiv \frac{C}{I_{mean}} > 0.5) \\ \left(\frac{c}{0.5}\right)^2 \frac{S_{ini}}{0.85C} \times i_{mean} + \left\{1 - \left(\frac{c}{0.5}\right)^2\right\} \times i & (c \equiv \frac{C}{I_{mean}} \leq 0.5) \end{cases} \quad \text{(B2)}$$

where i_{mean} [kg s^{-1}] is the mean annual inflow, i [kg s^{-1}] is the daily inflow, and c is the ratio of storage capacity to mean annual inflow. The first equation is for reservoirs with large storage capacity compared to annual inflow; release is independent of monthly inflow. The second equation is for reservoirs with small storage capacity compared to annual inflow. To avoid overflow and storage depletion during the year, release is influenced by daily inflow. The squared exponent and criterion of 0.5 are set empirically. When c is zero, reservoir operation is identical to run-of-the-river flow. If storage exceeds storage capacity even when allocated water has been released, the excess volume of water is also released.

If the reservoir's primary purpose is irrigation water supply, the "irrigation operation rule" is applied. This operation tries to reduce the interannual variation in streamflow. Daily release is not constant, but is controlled to be proportional to the daily water demand in the lower reaches. The annual total release for an operational year is identical to the case of nonirrigation reservoir operation. The water demand of irrigated areas is calculated for 10 grids downstream of a reservoir. The delay from delivery is not taken into account.

Acknowledgements. This study was supported by the Global Environmental Research Fund S-4 from the Ministry of the Environment, Japan, and JSPS/Grant-in-Aid for Scientific Research (S)19106008.

References

Alcamo, J., Döll, P., Henrichs, T., Kaspar, F., Lehner, B., Rosch, T., and Siebert, S.: Development and testing of the WaterGAP 2 global model of water use and availability, Hydrol. Sci. J., 48, 317–337, 2003a.

Alcamo, J., Döll, P., Henrichs, T., Kaspar, F., Lehner, B., Rosch, T., and Siebert, S.: Global estimates of water withdrawals and availability under current and future "business-as-usual" conditions, Hydrol. Sci. J., 48, 339–348, 2003b.

Alcamo, J., Florke, M., and Marker, M.: Future long-term changes in global water resources driven by socio-economic and climatic changes, Hydrol. Sci. J., 52, 247–275, 2007.

Arnell, N. W.: Climate change and global water resources, Global Environ. Chang., 9, S31–S49, 1999.

Arnell, N. W.: Climate change and global water resources: SRES emissions and socio-economic scenarios, Global Environ. Chang., 14, 31–52, 2004.

Baumgartner, A. and Reichel, E.: The world water balance, Elsevier Scientific Publishing Company, 182 p., 1975.

Gridded Population of the World Version 3 (GPWv3): Population Grids, available at http://sedac.ciesin.columbia.edu/gpw, last accessed on 28February 2007, 2005.

Döll, P. and Siebert, S.: A digital global map of irrigated areas, ICID J., 49, 55–66, 2000.

Döll, P. and Siebert, S.: Global modeling of irrigation water requirements, Water Resour. Res., 38, 1037, doi:10.1029/2001WR000355, 2002.

Döll, P., Kaspar, F., and Lehner, B.: A global hydrological model for deriving water availability indicators: model tuning and validation, J. Hydrol., 270, 105–134, 2003.

Department of Water Resources State of California: California Water Plan Update Bulletin, 160–98, 1998.

Dirmeyer, P. A., Gao, X. A., Zhao, M., Guo, Z. C., Oki, T. K., and Hanasaki, N.: GSWP-2 – Multimodel anlysis and implications for our perception of the land surface, B. Am. Meteor. Soc., 87, 1381–1397, 2006.

Doorenbos, J. and Pruitt, W. O.: Crop water requirements, FAO, Rome, 1977.

Food and Agriculture Organization: AQUASTAT: http://www.fao.org/ag/agl/aglw/aquastat/main/index.stm, 2007a.
Food and Agriculture Organization: FAOSTAT: http://faostat.fao.org/, 2007b.
Haddeland, I., Lettenmaier, D. P., and Skaugen, T.: Effects of irrigation on the water and energy balances of the Colorado and Mekong river basins, J. Hydrol., 324, 210–223, 2006a.
Haddeland, I., Skaugen, T., and Lettenmaier, D. P.: Anthropogenic impacts on continental surface water fluxes, Geophys. Res. Lett., 33, L08406, doi:10.1029/2006GL026047, 2006b.
Hanasaki, N., Kanae, S., and Oki, T.: A reservoir operation scheme for global river routing models, J. Hydrol., 327, 22–41, 2006.
Hanasaki, N., Kanae, S., Oki, T., Masuda, K., Motoya, K., Shen, Y., and Tanaka, K.: An integrated model for assessment of global water resources – Part 1: Input meteorological forcing and natural hydrological cycle modules, Hydrol. Earth Syst. Sci. Discuss., 4, 3535–3582, 2007, http://www.hydrol-earth-syst-sci-discuss.net/4/3535/2007/.
Hoekstra, A. Y. and Hung, P. Q.: Virtual water trade, A quantification of virtual water flows between nations in relation to international crop trade, IHE Delft, 2002.
Ishii, R., Nakaseko, K., and Takahashi, Y.: Agronomics, Asakura Publishing, 1999.
Japan River Association: Statistical yearbook of river discharge (in Japanese), Japan River Association, Tokyo, Japan, 2007.
King, J. M., Tharme, R. E., and de Villiers, M. S.: Environmental Flow Assessments for Rivers: Manual for the Building Block Methodology, Report No: TT 131/00, Water Research Commision, Pretoria, 2000.
Krysanova, V., Muller-Wohlfeil, D. I., and Becker, A.: Development and test of a spatially distributed hydrological water quality model for mesoscale watersheds, Ecol. Model., 106, 261–289, 1998.
Krysanova, V., Wechsung, F., Arnold, J., Srinivasan, R., and Williams, J.: SWIM (Soil and Water Integrated Model) User Manual, Potsdam Institute for Climate Impact Research, 2000.
Kundzewicz, Z. W., Mata, L. J., Arnell, N. W., Döll, P., Kabat, P., Jiménez, B., Miller, K. A., Oki, T., Sen, Z., and Shiklomanov, I. A.: Freshwater resources and their management, in: Climate Change 2007: Impacts, Adaptation and Vulnerability. Contribution of Working Group II to the Fourth Assessment Report of the Intergovernmental Panel on Climate Change, edited by: Parry, M. L., Canziani, O. F., Palutikof, J. P., v. d. Linden, P. J., and Hanson, C. E., Cambridge University Press, Cambridge, UK, 173–210, 2007.

Leff, B., Ramankutty, N., and Foley, J. A.: Geographic distribution of major crops across the world, Global Biogeochem. Cycles, 18, Gb1009, doi:10.1029/2003GB002108, 2004.
Meigh, J. R., McKenzie, A. A., and Sene, K. J.: A grid-based approach to water scarcity estimates for eastern and southern Africa, Water Resour. Manag., 13, 85–115, 1999.
Ministry of Land Infrastructure and Transportation: Handbook on minimum water level investigation (in Japanese), Ministry of Land Infrastructure and Transportation, Tokyo, Japan, 2001.
Neitsch, S. L., Arnold, J. G., Kiniry, J. R., Williams, J. R., and King, K. W.: Soil and water assessment tool, Theoretical Documentation, Version 2000, Texas Water Resources Institute, College Station, Texas, 2002.
Oki, T. and Sud, Y. C.: Design of total runoff integrating pathways TRIP - A global river channel network, Earth Interactions, 2, EI013, 1998.
Oki, T., Agata, Y., Kanae, S., Saruhashi, T., Yang, D. W., and Musiake, K.: Global assessment of current water resources using total runoff integrating pathways, Hydrol. Sci. J., 46, 983–995, 2001.
Oki, T. and Kanae, S.: Virtual water trade and world water resources, Water Sci. Technol., 49, 203–209, 2004.
Oki, T. and Kanae, S.: Global hydrological cycles and world water resources, Science, 313, 1068–1072, 2006.
Raskin, P., Gleick, P., Kirshen, P., Pontius, G., and Strzepek, K.: Comprehensive assessment of the freshwater resources of the world, Stockholm Environment Institute, 1997.
Shiklomanov, I. A.: Appraisal and assessment of world water resources, Water Int., 25, 11–32, 2000.
Shirakawa, N.: A conceptual framework for global estimation of environmental flow, Ann. J. Hydraul. Eng., 48, 421–426, 2004.
Shirakawa, N.: Global estimation of environmental flow requirement based on river runoff seasonality, Ann. J. Hydraul. Eng., 49, 391–396, 2005.
Smakhtin, V., Revenga, C., and Doll, P.: A pilot global assessment of environmental water requirements and scarcity, Water Int., 29, 307–317, 2004.
Smith, M.: CROPWAT – A computer program for irrigation planning and management, FAO, Rome, 1992.
Tan, G. X. and Shibasaki, R.: Global estimation of crop productivity and the impacts of global warming by GIS and EPIC integration, Ecol. Model., 168, 357–370, 2003.
Tennant, D.: Instream Flow Regimens for Fish, Wildlife, Recreation and Related Environmental

Resources, Fisheries, 1, 6–10, 1976.
Vörösmarty, C. J., Sharma, K. P., Fekete, B. M., Copeland, A. H., Holden, J., Marble, J., and Lough, J. A.: The storage and aging of continental runoff in large reservoir systems of the world, Ambio, 26, 210–219, 1997.
Vörösmarty, C. J., Green, P., Salisbury, J., and Lammers, R. B.: Global water resources: Vulnerability from climate change acid population growth, Science, 289, 284–288, 2000.
Williams, J. R.: The EPIC, in: Computer Models of Watershed Hydrology, edited by: Singh, V. P., Water Resources Publications, Littleton, CO, 909–1000, 1995.
World Agricultural Outlook Board U.S. Department of Agriculture: Major world crop areas and climatic profile, U.S. Department of Agriculture, 1994.
World Resources Institute (WRI): World Resources 1998–99, Oxford University Press, New York, 1998.

Table 1. Environmental flow requirement of Smakhtin et al. (2004). LFR indicates the low flow requirement [kg s^{-1}], HFR indicates the high flow requirement [kg s^{-1}], Q90 indicates 90th-percentile streamflow [kg s^{-1}], and Q_{mean} indicates mean annual streamflow [kg s^{-1}].

Classification	LFR	HFR	Annual environmental flow requirement (Q_{env})
$Q90<0.1Q_{mean}$	Q90	$0.20Q_{mean}$	$0.20Q_{mean} \le Q_{env} < 0.30Q_{mean}$
$0.1Q_{mean} \le Q90 < 0.2Q_{mean}$	Q90	$0.15Q_{mean}$	$0.25Q_{mean} \le Q_{env} < 0.35Q_{mean}$
$0.2Q_{mean} \le Q90 < 0.3Q_{mean}$	Q90	$0.07Q_{mean}$	$0.27Q_{mean} \le Q_{env} < 0.37Q_{mean}$
$Q90 \le 0.3Q_{mean}$	Q90	0	$0.30Q_{mean} \le Q_{env} < 0.50Q_{mean}$

Table 2. Environmental flow requirement of the environmental flow requirement module of the integrated model. The q indicates monthly runoff.

Description	Regional classification: Minimum monthly streamflow [mm mo^{-1}]	Regional classification: Maximum monthly streamflow [mm mo^{-1}]	Monthly environmental flow requirement (q_{env}): Condition [mm mo^{-1}]	Monthly environmental flow requirement (q_{env}): Monthly requirement
Dry (dry throughout a year)	$q_{min}<1$	$q_{max}<10$	$0\le q<1$ $1\le q$	$q_{env}=0$ $q_{env}=0.1\,q$
Wet (wet throughout a year) Stable (stable throughout a year)	$10\le q_{min}$ $1\le q_{min}$	$100\le q_{max}$ $q_{max}<100$		$q_{env}=0.3\,q+q_{flood}$ $q_{env}=0.1\,q$
Variable (dramatic change occurs between rainy and dry seasons)	Other than above		$0\le q<1$ $1\le q<10$ $10\le q$	$q_{env}=0$ $q_{env}=0.1\,q$ $q_{env}=0.3\,q+q_{flood}$

Table 3. Comparison of continental irrigation water withdrawal. Units: km^3 yr^{-1}.

Area (year)	This study (1995)	Döll and Siebert (2002)[1] (1995)	WRI (1998)[2] (1987)	FAO (2007) (2001)	Shiklomanov (1999) (1995)
Asia	2140	1880	1390	1940	1790
Europe	160	120	140	130	170
Africa	140	140	130	180	140
North America	240	190	200	200	200
South America	120	100	150	190	180
Oceania	20	30	10	20	20
Globe	2810	2450	2020	2660	2500

[1]Used in the global water resources assessment by Alcamo et al. (2003).
[2]Used in the global water resources assessment by Vörösmarty et al. (2000).

Table 4. Comparison of population under water-stressed conditions (withdrawal to water resources ratio [WWR]<0.4) with that from earlier studies. The stressed population is smaller than in earlier studies because of lower spatial resolution (consequently lower density, which alleviates water stress) and characteristics of the land–sea mask of GSWP2 (a large number of populous coastal grids are categorized as sea).

	This study	Vörösmarty et al. (2000)	Oki et al. (2001)
	(1.0°×1.0° grid-based)	(0.5°×0.5° grid-based)	(0.5°×0.5° grid-based)
Population [$\times 10^6$]	1250	1760	1700

Table 5. Effects of reservoir operation and environmental flow on the population under water stressed conditions. Units: million people.

	Reservoir operation Environmental flow	Enabled Enabled	Enabled Disabled	Disabled Enabled	Disabled Disabled
High stress	CWD≤0.5	2420	2160	2540	2290
Medium stress	0.5<CWD≤0.8	870	790	920	870
Low/no stress	0.8<CWD	1880	2210	1710	2010

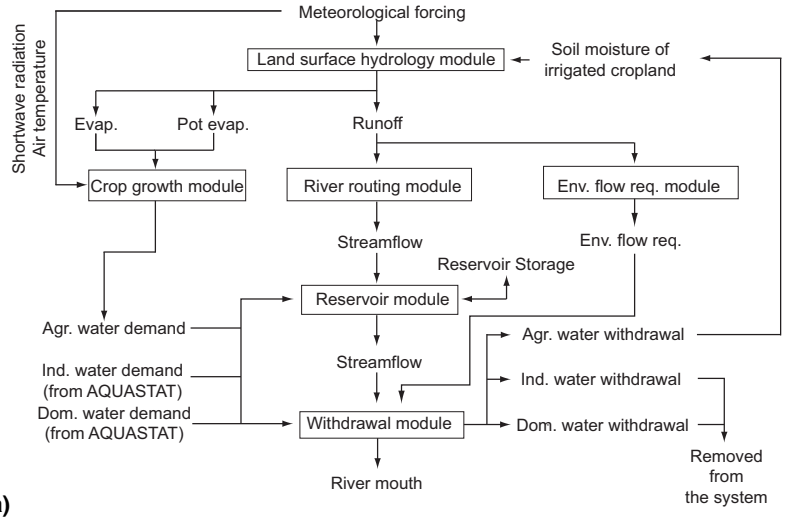

(a)

Fig. 1. Schematic diagram of water flow among modules.

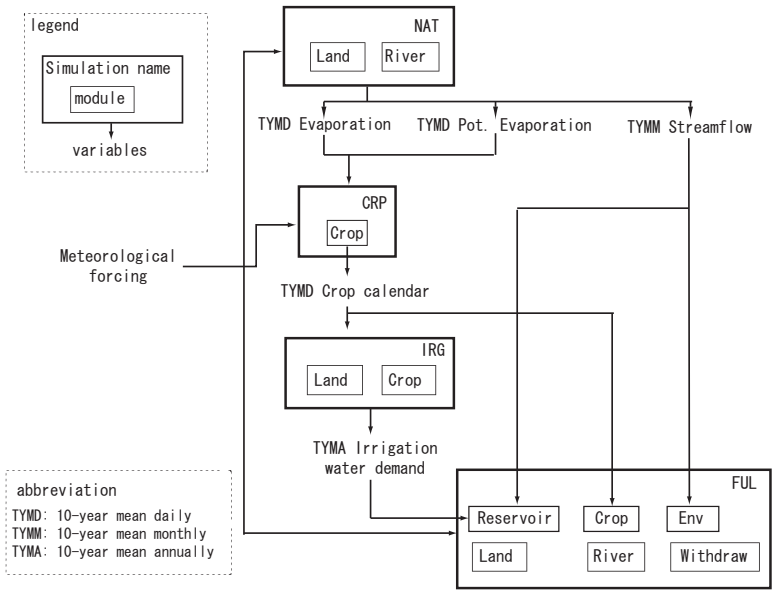

(b)

Fig. 1. Continued.

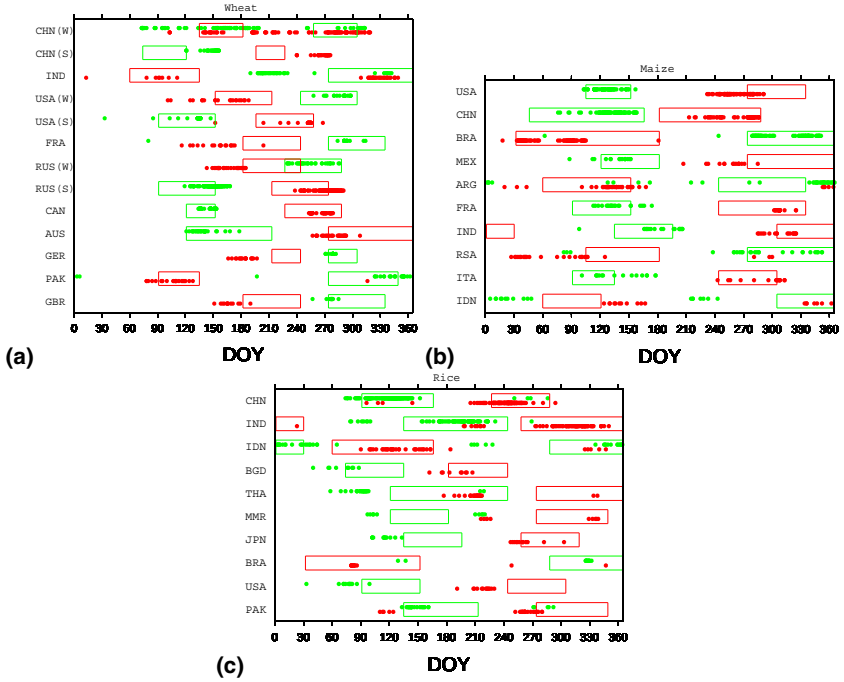

Fig. 2. Simulated planting and harvesting dates for **(a)** wheat, **(b)** maize, and **(c)** rice. The cropping calendars of 10 countries are shown for each crop with the largest production. Green plots show the simulated planting date for each grid; red plots show the harvesting date. Grids with >100 km^2 of cropland with >3% of the cropland occupied by the species were selected. Green boxes show the observed planting period; red boxes show the harvesting period (World Agricultural Outlook Board U.S. Department of Agriculture, 1994). In panel (a), (W) denotes winter wheat, and (S) denotes spring wheat.

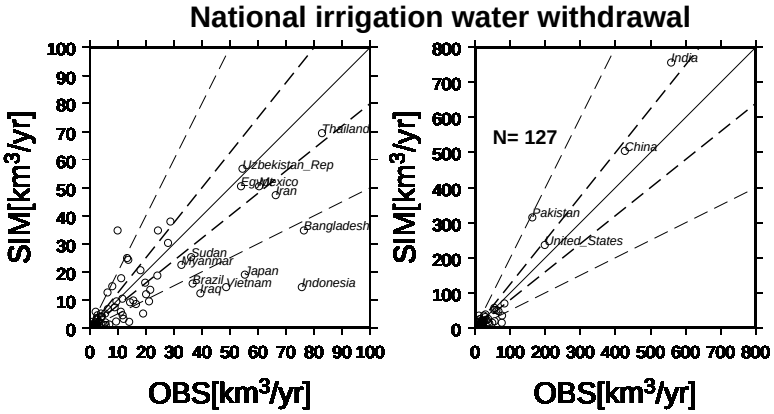

Fig. 3. Simulated irrigation water withdrawal for each country. The horizontal axis shows the reported value (Food and Agriculture Organization, 2007a) and the vertical axis shows the simulated value. The left panel shows countries with irrigation water withdrawal <100 $km^3\ yr^{-1}$, the right panel shows all plots.

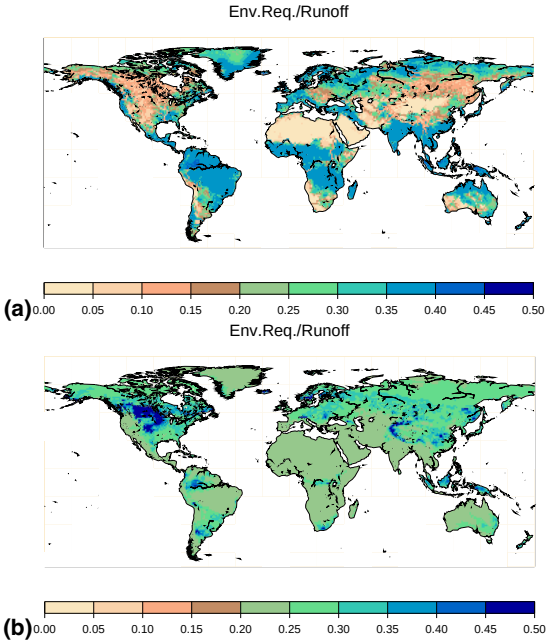

Fig. 4. Distribution of the ratio of estimated annual environmental flow requirement to annual total runoff (both grid-based). **(a)** This study and **(b)** Smakhtin et al. (2004).

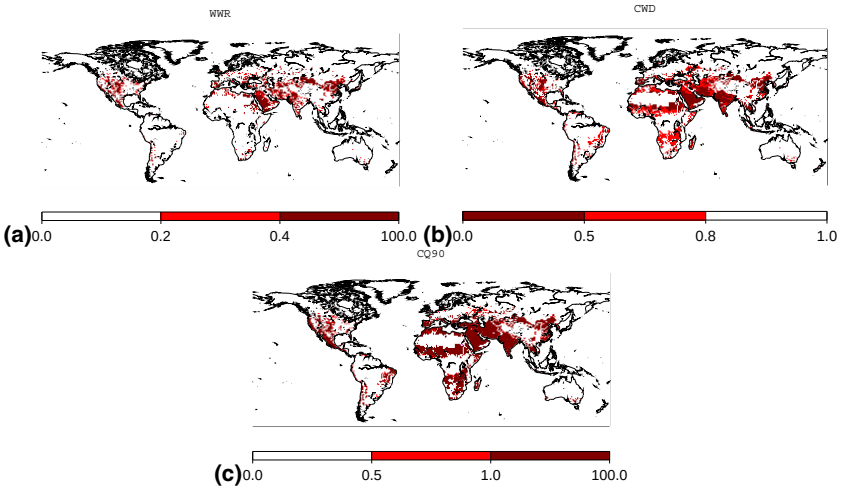

Fig. 5. Distribution of water-scarce areas. **(a)** Conventional withdrawal to water resources ratio (WWR; on an annual basis); **(b)** newly devised cumulative supply to demand ratio (CWD; on a daily basis); **(c)** consumptive water withdrawal to Q90 ratio (CQ90; on an annual basis). To distinguish water-scarce areas of highly populated areas from those of less populated areas (i.e., desert), grids with <1 person km^{-2} were eliminated from the calculations.

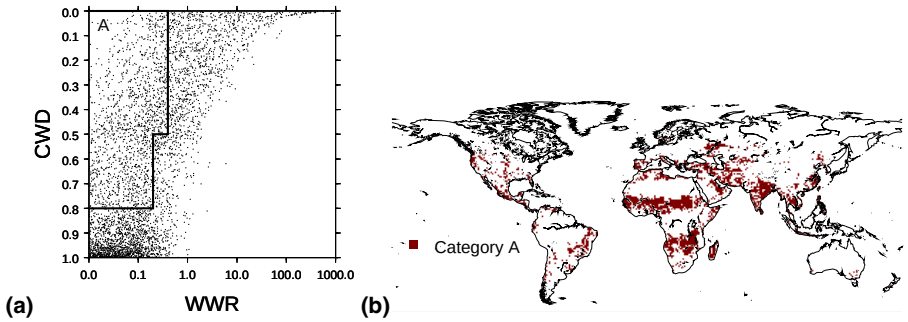

Fig. 6. The relationship between the withdrawal to water resources ratio (WWR) and the cumulative supply to water demand ratio (CWD). **(a)** Scattergram of WWR and CWD for all calculated grid cells (total of 15 238). Category A shows the plots in which WWR indicates low to no stress ($0 \leq WWR < 0.2$) but CWD indicates medium to high stress ($0 \leq CWD < 0.8$) or WWR indicates medium stress ($0.1 \leq WWR < 0.4$) but CWD indicates high stress ($0 \leq CWD < 0.5$). **(b)** Geographical distribution of plots in categories A.

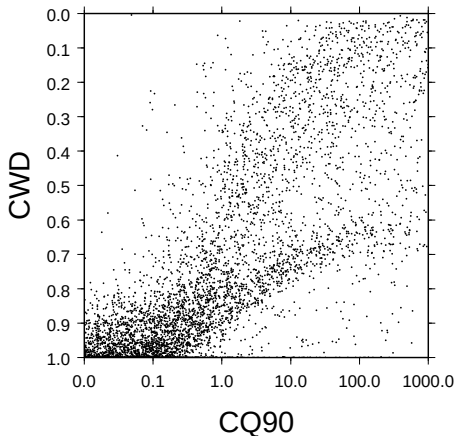

Fig. 7. The relationship between the consumption to Q90 ratio (CQ90) and the cumulative withdrawal to water resources ratio (CWD).